Korean J. Chem. Eng., 33(6), 1757-1766 (2016)
DOI: 10.1007/s11814-016-0041-6
pISSN: 0256-1115
eISSN: 1975-7220

INVITED REVIEW PAPER

Recent developments in scale-up of microfluidic emulsion generation via parallelization

Heon-Ho Jeong*, David Issadore,***, and Daeyeon Lee*,†**

*Department of Chemical and Biomolecular Engineering, University of Pennsylvania, Philadelphia, Pennsylvania 19104, U.S.A.
**Department of Bioengineering, University of Pennsylvania, Philadelphia, Pennsylvania 19104, U.S.A.
***Electrical and Systems Engineering, School of Engineering and Applied Science,
University of Pennsylvania, Philadelphia, Pennsylvania 19104, U.S.A.
(*Received 21 December 2015 • accepted 4 February 2016*)

Abstract−Microfluidics affords precise control over the flow of multiphasic fluids in micron-scale channels. By manipulating the viscous and surface tension forces present in multiphasic flows in microfluidic channels, it is possible to produce highly uniform emulsion droplets one at a time. Monodisperse droplets generated based on microfluidics are useful templates for producing uniform microcapsules and microparticles for encapsulation and delivery of active ingredients as well as living cells. Also, droplet microfluidics have been extensively exploited as a means to enable high-throughput biological screening and assays. Despite the promise droplet-based microfluidics hold for a wide range of applications, low production rate (<<10 mL/hour) of emulsion droplets has been a major hindrance to widespread utilization at the industrial and commercial scale. Several reports have recently shown that one way to overcome this challenge and enable mass production of microfluidic droplets is to parallelize droplet generation, by incorporating a large number of droplet generation units (N>>100) and networks of fluid channels that distribute fluid to each of these generators onto a single chip. To parallelize droplet generation and, at the same time, maintain high uniformity of emulsion droplets, several considerations have to be made including the design of channel geometries to ensure even distribution of fluids to each droplet generator, methods for large-scale and uniform fabrication of microchannels, device materials for mechanically robust operation to withstand high-pressure injection, and development of commercially feasible fabrication techniques for three-dimensional microfluidic devices. We highlight some of the recent advances in the mass production of highly uniform microfluidics droplets via parallelization and discuss outstanding issues.

Keywords: Microfluidics, Emulsions, Droplets, Scale-up, Large-scale Integration, Device Fabrication

INTRODUCTION

Microfluidics is the science and technology of precise manipulation of fluids in micro-scale channels. The early applications of microfluidics include single-phase fluids for chemical reaction/analysis and fluid rheology, which allow the use of small volumes of samples and rapid analyses [1,2]. Microfluidic technology has also enabled unprecedented control over flows involving multiphasic fluid mixtures, which has been used to generate highly monodisperse emulsion droplets. Such a development has led to the advent of droplet-based microfluidics. The most distinguishing and unique features of droplet-based microfluidics are precise formation and manipulation of droplets allowing for high speed droplet generation, mixing, separation, split and coalescence [3-7].

Droplet formation units can be classified into T-junctions and flow-focusing channels. In each of these configurations, a dispersed fluid phase is compartmentalized into many small droplets in the continuous fluid phase by the balance between the shear and surface tension forces. During droplet formation, the interplay of different forces, as represented by dimensionless numbers such as Capillary (ratio of viscous force and interfacial tension) and/or Weber numbers (ratio of inertial force and surface tension force), affects the dynamics of droplet formation [8,9]. The generated monodisperse droplets from microfluidics are useful templates for producing monodisperse microcapsules and microparticles for the encapsulation and delivery of active ingredients such as drugs, nutrients and fragrances as well as living cells [10-12]. In these applications, uniformity can provide several advantages such as the synthesis of highly uniform particles and gas bubbles for biomedical applications where delivery of precise amounts of an active ingredient is critical. In addition, uniform droplets that range in volume from femtoliter to nanoliter have been used as isolated microreactors for enzyme reactions, digital polymerase chain reaction (PCR), and nanoparticle synthesis [13-17]. Moreover, compartmentalization of a large number of liquid and solid samples into many picoliter droplets has been used for high-throughput screening [18-21].

Despite these promising demonstrations in high throughput screening and materials synthesis, droplet production rate in a single microfluidic unit remains low, which has limited the translation of the laboratory-scale success to commercial-scale production and manufacturing. A typical single droplet generator can produce in the range of 0.1-10 mL/hour of emulsion droplets with extremely narrow size distribution (typically, the coefficient of variation (C.V.) is less than 5%), whereas much greater scale (well above L/hour) is

†To whom correspondence should be addressed.
E-mail: daeyeon@seas.upenn.edu

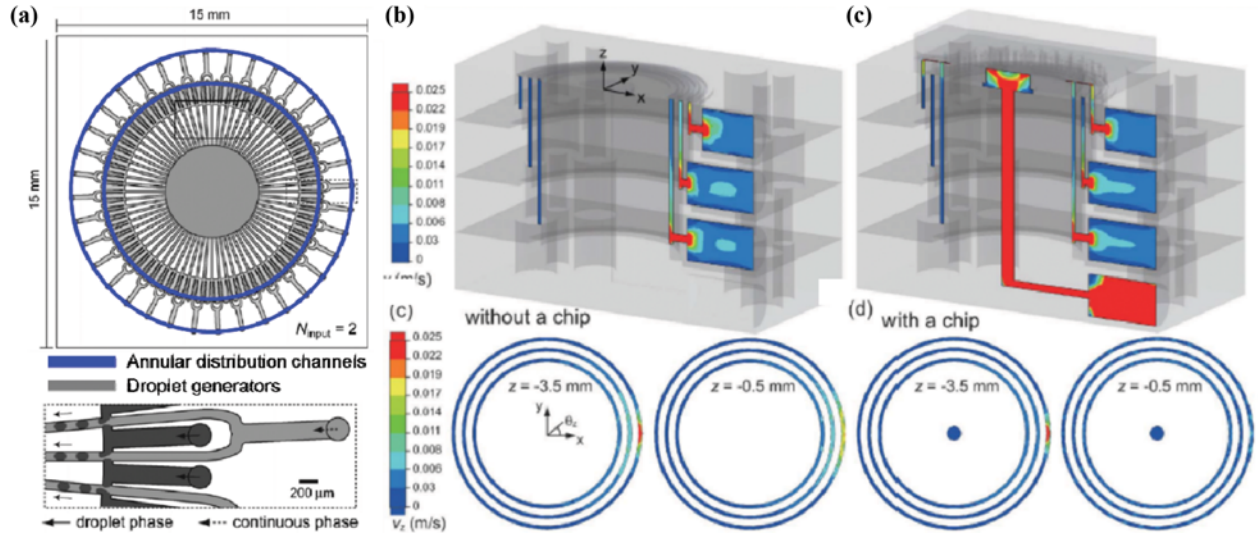

Fig. 1. Microfluidic channel design for uniform distribution of fluids. (a) Schematic diagram for circular array of 144 droplet generators. (b) Three-dimensional flow simulation in a module having distribution channels when microfluidic chip is disconnected. Large variations are observed in channels. (c) In the presence of microfluidic chip, the variations are dramatically reduced in distribution channels due to higher channel resistance. Reproduced by permission of The Royal Society of Chemistry [28].

required for commercial-scale manufacturing [22,23]. Conventional emulsification methods (high-speed blenders, mills, and ultrasonic homogenizers) that apply high shear force to a large volume of two immiscible phases can produce emulsions at the rate of 100-20,000 L/hour; however, the produced droplets have wide size distributions with C.V. well above 30% [24]. Thus, to ensure that multiple areas benefit from the use of droplet-based microfluidics, it is imperative to enable the scale-up of droplet generation [23,25-27]. One possible solution is the large-scale parallel integration of droplet generation units, enabling the use of single-set of injection ports; that is, a large number of droplet generators are incorporated onto the same chip and fluid is distributed to these generators from a single set of fluid inlets. Due to the large number of droplet generators (N~1,000) needed to attain commercially relevant flow rates (>1 L/hr), three-dimensional channels are required to implement this parallelization.

In this review, we highlight recent advances in the fabrication of three-dimensional microfluidic devices to enable mass production of uniform emulsion droplets. As will be discussed below, several critical considerations should be made, including the design of channel geometries to ensure even distribution of fluids to each droplet generator, methods for large-scale and uniform fabrication of microchannels, device materials for mechanically robust operation to withstand high-pressure fluid injection, and development of commercially feasible fabrication techniques for three-dimensional microfluidic devices. We also discuss some of the outstanding challenges to further translate droplet-based microfluidics into the industrial scale production of emulsions.

PARALLELIZATION OF DROPLET GENERATION

To achieve parallelization of droplet formation, three-dimensional channel geometries are essential to integrate both droplet generators and the fluid channels that distribute fluid to each generator from a single set of fluid injection ports. A typical parallel droplet generation microfluidic device is composed of three layers, including a droplet generation layer, a delivery layer, and an intermediate layer. The intermediate layer having through-holes connects the generation layer and the delivery layer. From a single set of inlets for the fluid phases (e.g., oil and water), fluids are distributed to the droplet generators via distribution channels and through-holes. The most important consideration is that the flow rates of the two fluids in all of the generators should be kept even and uniform to ensure a narrow dispersion of droplet size.

Two most common designs used for distribution channels are ladder-like geometry and tree-like branched geometry. The ladder geometry has main distribution channels for the fluid phases, which are connected to droplet generators (Fig. 1(a)). Nisisako et al. simulated such a three-dimensional flow to evaluate the fluid velocity in annular distribution channels that have 30,000 times larger cross-sectional area than that of droplet generator channels [28]. The results show uneven fluid distribution in annular distribution channels without droplet generators (Fig. 1(b)). In contrast, the distribution channels that are coupled to droplet generators show more uniform distribution of the fluids (Fig. 1(c)). This finding indicates that the microchannel dimension significantly affects the uniform distribution of fluids.

A recent study has proposed a quantitative approach to achieve uniform flow rates across all of the generators in the ladder-like geometry. It was shown that the hydraulic resistance of delivery channel (R_d) between two adjacent droplet generators should be much less than that of the droplet generators (R_g) (Fig. 2). The hydraulic resistance for laminar flow through a rectangular channel can be estimated using the following equation [28,29],

$$R = 12\frac{\mu l}{wh^3}\left(1-0.63\left(\frac{h}{w}\right)\right)^{-1} \quad (1)$$

where μ is the dynamic viscosity of the fluid and w, h, and l are

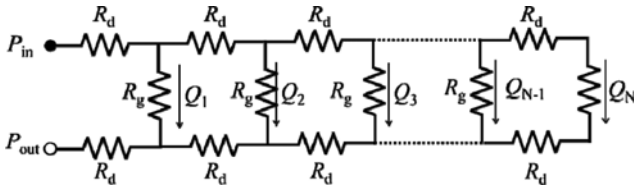

Fig. 2. A model for hydraulic resistances in the ladder-like network of channels. R_d indicates the resistance of distribution and collection channels, and R_g indicates the resistance of droplet generator channel.

the width, height, and length of the channel, respectively. The aspect ratio is used as either height/width or width/height such that 0≤ (h/w or w/h) ≤1. Assuming that there are two droplet generators that are connected in parallel, the ratio of flow rates in two droplet generators can be expressed as $Q_1/Q_2=1+2(R_d/R_g)$. The two droplet generators would have essentially the same flow rates when the ratio of the resistances becomes negligible (e.g., $R_d/R_g<<0.01$); in other words, the maximum difference in flow rates between the two generators is $2(R_d/R_g)$. In the presence of N number of droplet generators (R_{g1}, R_{g2}, R_{g3}, ···, R_{gN}), this argument can be modified that to keep the flow rates of the fluids in all of the generators uniform, the following inequality has to be satisfied,

$$2N_g\left(\frac{R_d}{R_g}\right)<0.01 \quad (2)$$

where R_d is the fluidic resistance along the delivery channel between each droplet generators, R_g is the fluidic resistance of individual droplet generators, and N_g is the number of droplet generators in each row. Using this argument, ladder-like channels can be designed to give uniform flow rates of the fluids in all N_g generators. Several reports have shown that highly uniform emulsion droplets ranging in size between 45.0 and 90.7 μm can be produced at the production rates ranging from 8 and 1,500 ml/hr [28,30,31].

The tree-like branched channel network, as shown in Fig. 3, has the advantages of evenly and symmetrically dividing fluids in branched channels and increasing the number of droplet generators starting from one set of inlets without the need to consider the hydrodynamic resistance of each channel [32,33]. And a recent report demonstrated a device with 512 parallel generators by three-dimensional stacking of droplet generators, enabling 1 L/hour production rate of 100 μm emulsion droplets [34]. Although the design and implementation of tree-like branched geometry have the advantage of simplicity, the ladder-like geometry offer two significant advantages over tree-like geometry. In typical tree-like branched geometry, a significant space has to be invested in the placement of the branches. In contrast, it is possible to design a two-dimensional array of droplet generators with extremely high density using the ladder geometry. A recent study showed that 1,000 droplet generators could be placed on a 6.0×5.0 cm^2 area. In the ladder geometry, if the resistance ratio of the delivery channel and droplet generator is sufficiently large, fluid distribution is not significantly affected by a droplet generator becoming clogged. In the tree geometry, however, clogging of one channel in the branched channels significantly affects the flow distribution due to the breaking of symmetry [35]. One consideration that has not been accounted for in the generation of emulsions using parallel devices is the deformation of PDMS microchannels under high pressure. While it has been recognized that the deformation of a single droplet generator can affect the emulsion uniformity [7], currently little is understood on how channel deformation would affect the droplet formation in parallel devices, which warrants future investigation.

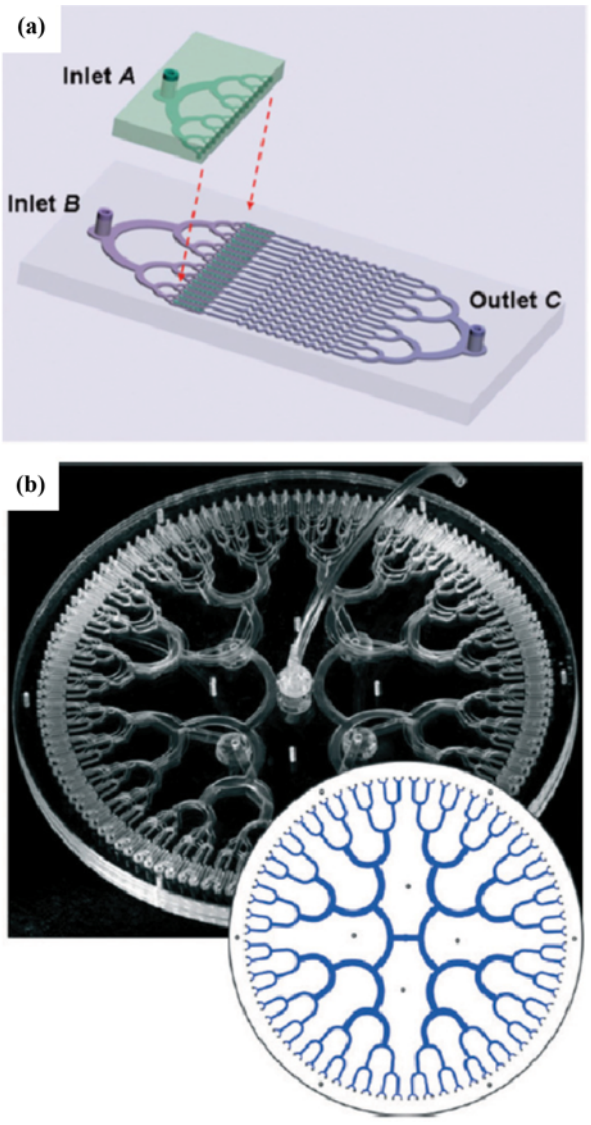

Fig. 3. Tree-like branched distribution channels for parallelization of droplet generators. (a) A simple two-dimensional tree-like distribution channel connected to 16 droplet generators. (b) A fractal three-dimensional tree-like distribution channel for connecting 128 droplet generators. Reproduced by permission of The Royal Society of Chemistry [33,34].

MATERIALS AND FABRICATION METHODS FOR PARALLEL MICROFLUIDIC DEVICES

A microfluidic device for mass production of emulsion drop-

lets can be fabricated using different techniques and materials [36-38]. Because the mass production of microfluidic droplets typically requires the use of a complex three-dimensional channel geometry, it is important to understand the advantages and disadvantages of each method and material that is used for microfluidic channel fabrication. Prudent selection of methods and materials will enable the fabrication of densely packed generators with high repeatability, reliability and precision. In this section, we summarize different materials and fabrication techniques that have been used to prepare microfluidic devices for the mass production of emulsions and discuss the advantages and disadvantages of each material and method. In particular, we discuss different methods that have been used to bond different layers that are separately prepared to form three-dimensional channels. Bonding is extremely critical as misalignment of channels in different layers and incomplete bonding would significantly degrade the performance of the parallel device.

1. Deep Reactive Ion Etching (DRIE) for Glass Microfluidic Chips

A well-established method for micro-processing of glass and silicon is deep reactive ion etching (DRIE), which is capable of etching rectangular trenches using gas precursors such as SF_6, C_4F_8, CF_4, or CHF_3. Masking layer such as electroplated Ni, amorphous silicon, or SU-8 photoresist is required to selectively etch glass. Nisisako et al. have used synthetic silica glass for mass production of droplets in a device with 256 parallel generators (50-200 μm width and 100 μm depth) formed by DRIE [28,39].

One of the biggest challenges in making a three-dimensional glass microfluidic device is bonding different layers that have been separately prepared via DRIE. Two representative methods of bonding are plasma-activated bonding and fusion bonding. Plasma-activated glass-glass bonding is achieved by nitrogen radical activation onto glass surfaces in a microwave reactor after an oxygen RIE treatment. An annealing at 400 °C is required to achieve a bonding strength of 24 MPa, which may not be enough for high pressure injection that is required for mass production of emulsions [40,41]. Glass-glass fusion bonding has been developed to enhance the bond strength. At a high temperature of 650 °C or above, glass becomes soft and two glass surfaces can be brought to form conformal contact. Three-dimensional glass devices made using the fusion bonding method, which can readily withstand high flow pressures, have been used for the high-throughput production of uniform emulsions [42-44]. Alignment between droplet generators and distribution channel was achieved using micromachined stainless-steel supporting holders that have cylindrical distribution channels and holes in each layer to fit with the microfluidic chip (Fig. 4). This glass-based microfluidic chip has achieved production rates as high as 180 mL/hour for O/W emulsion.

Although glass microfluidic chips have several advantages, such as great mechanical and chemical properties (e.g., solvent resistance, easy chemical modification, high mechanical strength, and thermal stability), device fabrication is time-consuming, laborious and complex. The etch rate is extremely low (0.5-0.8 μm/min) and the selectivity can be poor [45,46]. Glass-glass bonding techniques generally require an extremely clean environment, specialized tools, and high temperature bonding. Also, the fabrication of through-

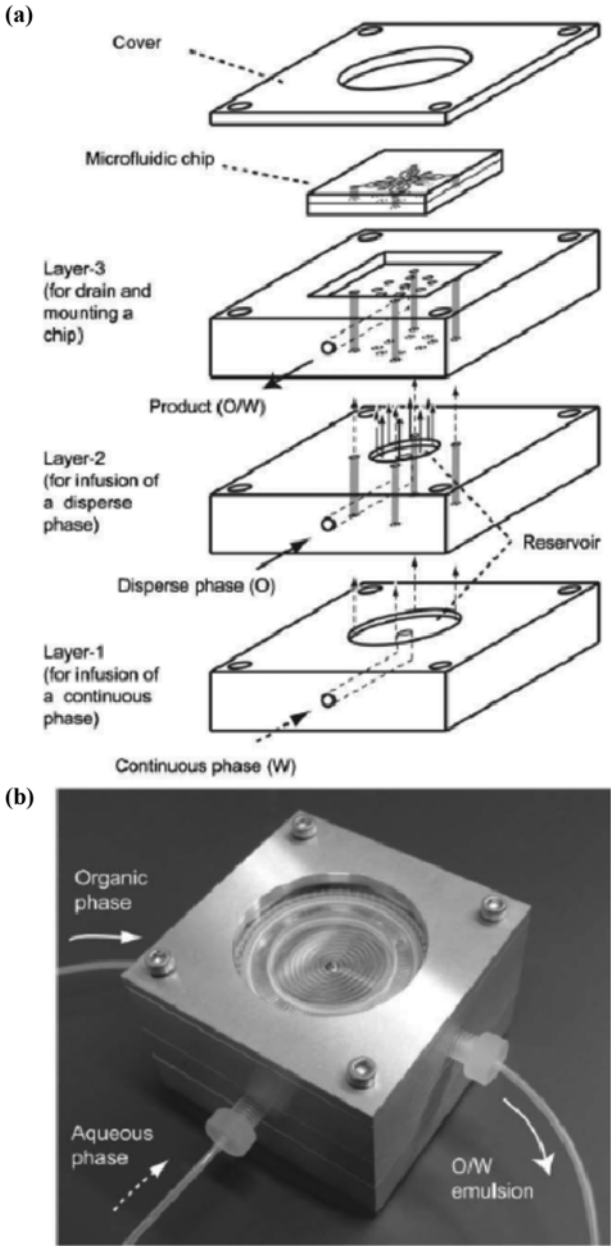

Fig. 4. A glass microfluidic chip for mass production of emulsions. (a) Schematic diagram of 3D view for assembly and alignment between supporting holders and microfluidic channels. (b) Photograph of a finalized device for high-throughput production. Reproduced by permission of The Royal Society of Chemistry [39].

holes for fluidic ports requires additional equipment such as sandblaster and drill.

2. Plastic-based Microfluidic Channels Via Micromilling

Thermoplastics such as polymethylmethacrylate (PMMA) and polycarbonate (PC) have become quite popular for the fabrication of microfluidic devices. Although their thermal and chemical compatibility may not be as high as those of glass, plastics are much easier to process and also have quite excellent mechanical properties with higher toughness than glass. Most common processing meth-

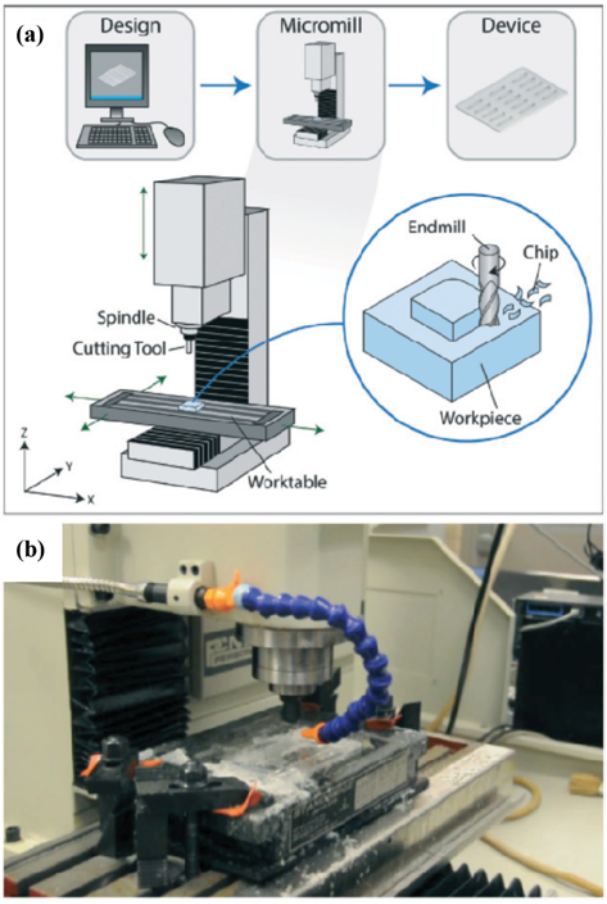

Fig. 5. Microlling machine for plastic processing. (a) Schematic diagram for operation procedure and components of CNC milling. (b) A photograph for operation of CNC milling machine. Reproduced by permission of The Royal Society of Chemistry [50].

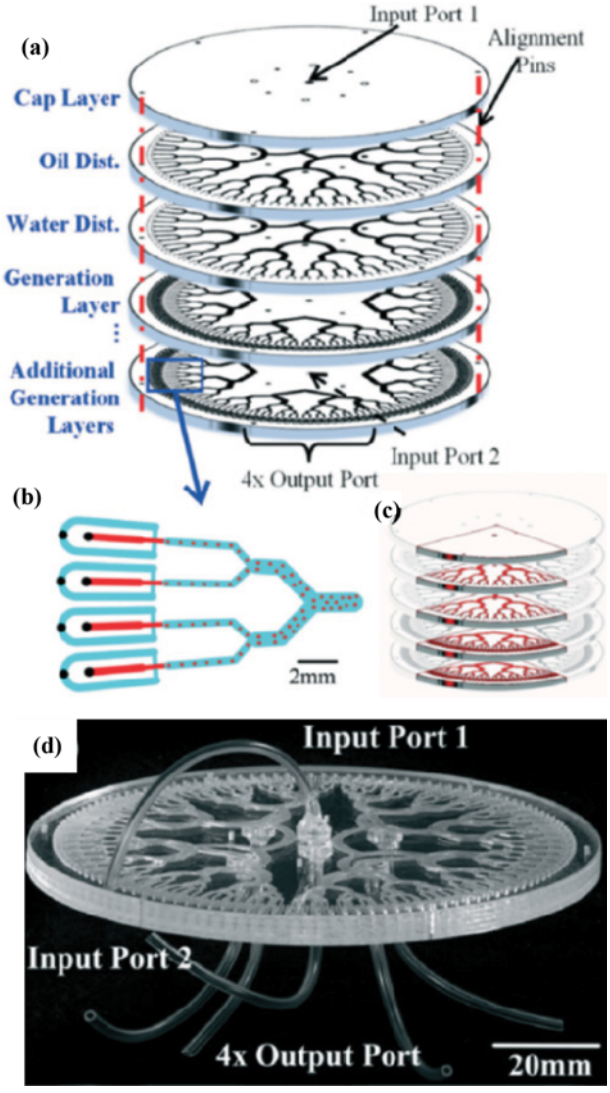

Fig. 6. Three-dimensional parallel device made with PMMA. (a) A schematic diagram of device composed of cap layer, oil and water distribution layers, and generation layers in three dimensional layer. (b) Parallel flow focusing droplet generators in a generation layer. (c) Sharing inputs and output between aligned layers. (d) Photograph of the entire PMMA device having 256 droplet generators. Reproduced by permission of The Royal Society of Chemistry [34].

ods for plastics are injection molding, hot embossing, and micromilling [47-49]. Among them, computer numerical control (CNC) micromilling is widely used for microfluidic channel fabrication due to ease of use and simple manufacturing process [50,51]. The CNC micromilling can precisely execute x-y plane movement at a resolution of ±0.5 μm and vary the rotating speed of cutting tools. CNC micromilling automates the machining process and therefore enables rapid prototyping, enhanced repeatability and precise channel formation with reduced human error (Fig. 5). CNC milling is capable of fabricating devices with features down to several micrometers in size.

Conchouse et al. have used CNC milling to prepare PMMA microchannels (~250 to 2,000 μm±0.5 μm width and ~100 to 300 μm±10 μm depth) with 512 parallel droplet generators [34]. This device consists of three layers: a layer with fractal tree-like distribution channel, a layer with 128 flow-focusing droplet generators, and a layer with interconnection holes, which can be easily fabricated via CNC drilling. Care must be taken in using CNC milling machining because the process can lead to rough surfaces, which can result in inaccurate fluid flows and bonding inhibition. The three layers prepared via CNC milling were stacked with the aid of alignment pins (Fig. 6). Subsequently, simultaneous heat (over glass transition temperature) and compression is applied to the stacked and aligned PMMA layers for thermal fusion bonding. The thermal fusion bonding can be applied to various thermoplastic materials in a straightforward manner, and it gives relatively high bonding strengths [52-55]. This PMMA device can withstand maximum operating pressure of 7.5 bar and produces emulsion at the rate of up to 1 L/hour. One challenge in the use of high-temperature fusion bonding is that the procedure can induce channel deformation and collapse, which makes it difficult to use small channels that are below 100 μm [56,57]. Recently, plasma, UV, or UV/ozone assisted surface modification has been developed for low-temperature bonding; however, these methods do not provide enough bonding strength

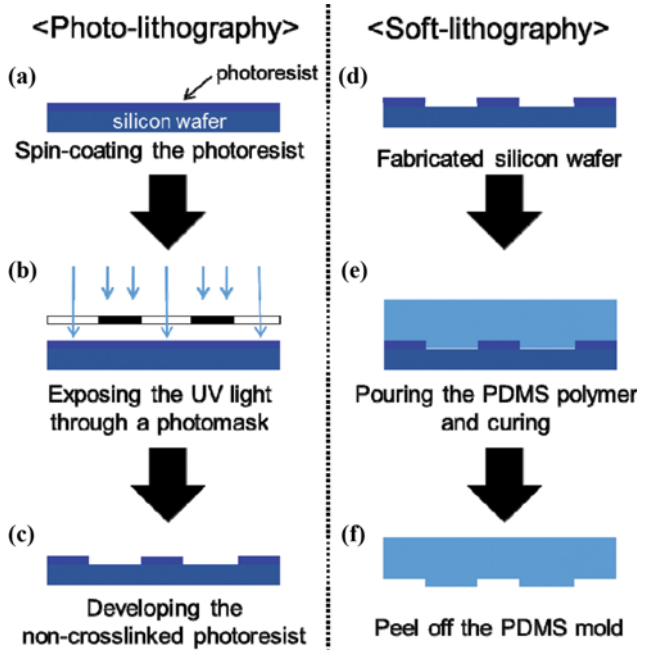

Fig. 7. Schematic illustration of photo-/soft-lithography. (a)-(c) Preparation procedure of silicon master by photo-lithography. (a) Thin photoresist coated on silicon wafer by spin-costing, (b) selective UV irradiation through photomask, and (c) final silicon master with micropatterns after removing un-crosslinked photoresist. (d)-(f) Preparation procedure of PDMS mold by soft-lithography. (d) Prepared silicon master with desired design, (e) pouring PDMS precursor, and (f) peeling off the PDMS mold/channel after solidification of PDMS polymer.

that is necessary to prepare three-dimensional channels that can withstand high pressure typically present in large-scale production of emulsions [58,59].

3. Soft Elastomer Devices Via Photo-/Soft-lithography

One of the most widely used methods for the fabrication of microchannel is photo- and soft-lithography [36,60]. Photo-lithography is used to fabricate micropatterns on a silicon wafer, which becomes a master for soft-lithography. To fabricate masters with microscale patterns, a spin-coated photoresist layer is selectively exposed to the UV light through a photomask, and a developing reagent is used to dissolve the non-crosslinked photoresist regions (Fig. 7(a)). Microchannel resolution depends on the types of photomask (>5 μm width) and photoresist (>1 μm height). Fabrication process for the master is complex, and specialized facilities such as a clean room are required. However, once a master mold is prepared, an elastomer such as polydimethylsiloxane (PDMS) can be used to easily replicate the features of the silicon master. PDMS in its liquid state is poured onto the hard master and subsequently cured to form the PDMS channel. The low surface free energy and elasticity of soft PDMS allow easy release of cured PDMS from the silicon master. PDMS replica can be repeatedly fabricated from a single silicon master without damage to the photoresist patterns, thus making rapid prototyping feasible (Fig. 7(b)).

In contrast to bonding of hard materials such as glass and thermoplastics, a piece of PDMS can be readily bonded to another piece of PDMS or glass substrates without high temperature and/or pressure application because of their tendency to form conformal contact [61,62]. Simple activation of the PDMS surface with O_2 plasma creates hydroxyl groups that will form covalent bonds when they come in contact with hydroxyl groups on another surface. Bond strength can be further enhanced by using the so-called partial curing method, in which two partially cured PDMS pieces are brought in contact with each other and bonded by thermal curing. Un-reacted prepolymers on both surfaces undergo cross-linking. Muluneh et al. have fabricated a PDMS device with 512 parallel flow-focusing droplet generators that are connected by ladder-like distribution channels using a combination of soft-lithography, laser machining and partial curing [30]. This device also consists of three layers: distribution layer, interconnection layer and droplet generation layer. Due to high resolution fabrication of microchannel that is feasible via photo-/soft-lithography, they have been able to achieve a high density 2D array of 512 droplet generators on a 9 cm^2 area. Laser micromachining [63], which can process various substrates including glass as well as hard and soft polymers, was used to form large features such as distribution channels (380 μm width and 500 μm height) and through-holes (300 μm diameter). By integrating 512 droplet generators, water-in-oil droplets were produced at the flow rates of 8 ml/hour for the dispersed phase and 20 ml/hour for the continuous phase. One of the key challenges in making PDMS-based three dimensional channels is that the three layers have to be bonded while ensuring the alignment of channels in the three layers. Because PDMS is very adhesive, once the surface of a PDMS layer touches the surface of another PDMS, it becomes exceedingly difficult to separate, realign and bond these layers. Thus the repeatability of channel fabrication is not very high.

To overcome this technical challenge, our group has recently developed a three-dimensional monolithic elastomer device (3D MED) via a double-sided imprinting method, which uses a combination of a multi-height hard master and an elastomer-based soft master [31]. The multi-height hard master contains the channels for the droplet generation and through-hole layers, whereas the soft master has the features for the distribution channels. The two masters are brought into contact with each other with uncured liquid-state PDMS in between them. PDMS functions as lubricant, making it extremely easy to align the features in the two masters. Once PDMS is cured, the two masters are separated, releasing a 3D MED. The hard and soft masters used in double-sided imprinting are reusable and cost effective. By using the double-sided imprinting method, a high density 2D array of 1,000 droplet generators on 30 cm^2 area was achieved in 3D MED (Fig. 8). Also, since the device is fabricated from a single piece of PDMS, it can withstand extremely high pressure (P~100 psi) and we have achieved production rates as high as 1.5 L/hour (>30 billion 45 μm diameter droplets per hour) in a device with 1,000 parallel flow-focusing generators, which to our knowledge is the highest volumetric production rate per unit area of device to date.

4. 3D Printing-based Microfluidic Channels

Recently, three-dimensional (3D) printing has become one of the most powerful rapid prototyping processes in a wide range of research areas. 3D printing directly produces user-designed struc-

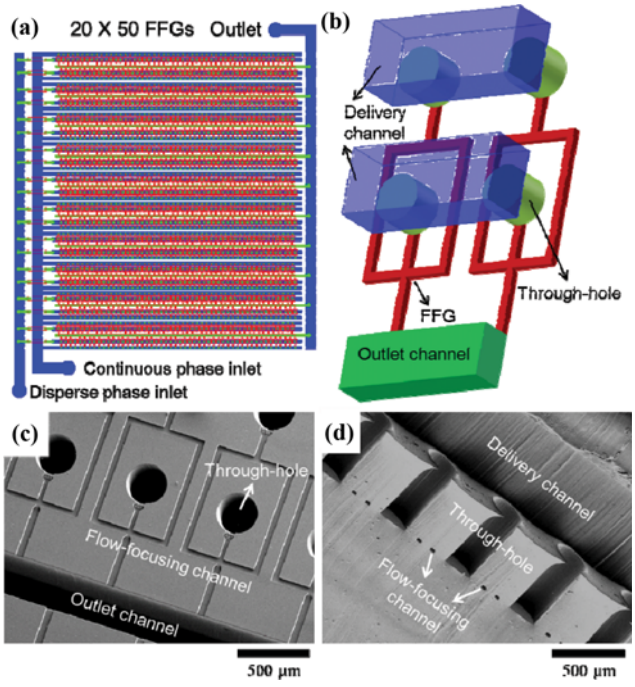

Fig. 8. Three-dimensional monolithic elastomer device (3D MED) for kilo-scale droplet generation. (a) Schematic diagram of 3D MED design having 1,000 droplet generators. (b) Detailed flow-focusing generators connected to delivery channels for parallel distribution of solutions. (c) and (d) SEM images for flow-focusing generators connected to through-holes and outlet channel. Reproduced by permission of The Royal Society of Chemistry [31].

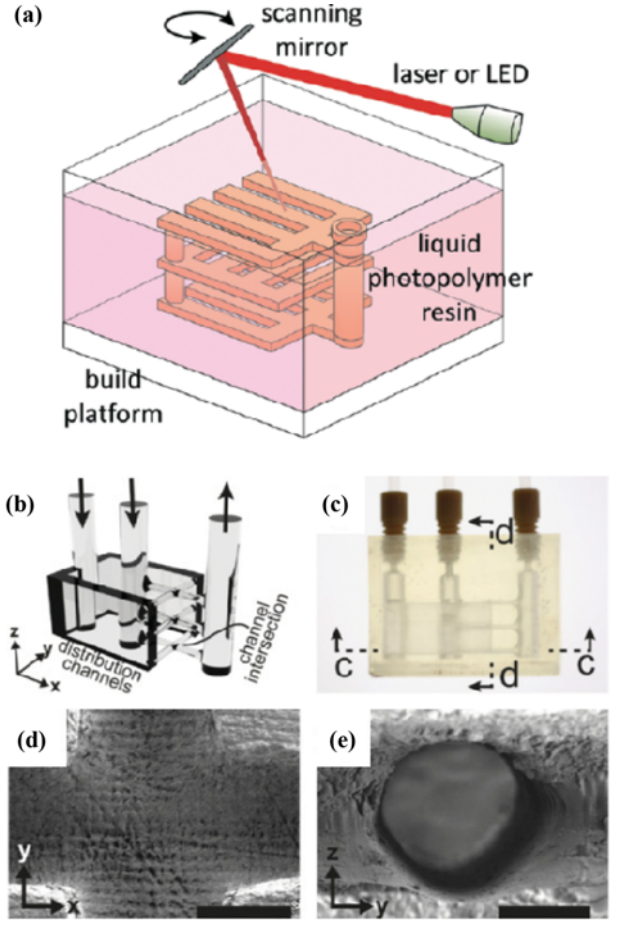

Fig. 9. 3D printed parallel droplet generators device. (a) Schematic diagram for fabrication of 3D microchannel by 3D printing. (b) Rendered 3D microchannel with parallel droplet generators. (c) Photograph of 3D printed device connected to two inlets and one outlet tubes. (d) and (e) SEM images of cross-section for channel intersections. Reproduced by permission of The Royal Society of Chemistry [50] and Reproduced with permission from [72] Copyright [2015] American Chemical Society.

tures in a fully three-dimensional space without intense labor and complex procedures (Fig. 9(a)). Thus, procedures such as alignment and bonding of multiple layers can be completely eliminated. Naturally, this approach is currently being used for the direct fabrication of 3D microfluidic devices [64-71]. Femmer et al. have fabricated a 28-droplet generator-parallelized 3D microfluidic device (70 cm^2) using digital light processing that allows vertical stacking of individual flow-focusing generators (Fig. 9(b)-(e)) [72]. A hydrophobic methacrylate-based photoresist was used to fabricate the device in a layer-by-layer fashion by selective photo-crosslinking. By this technique, each layer contributes a fixed voxel-height to the three-dimensional structure. Using this device, 500 μm monodisperse emulsions and microgels were produced at the rate of 3 L/hour. Although 3D printing has the highest potential for scalable production of microfluidic devices with complex geometry, spatial resolution of commercial printers is currently limited to features that are larger than 200 μm.

CONCLUSION

We have highlighted recent advances in the parallelization of droplet generators in three-dimensional microfluidic devices for large-scale production of emulsion droplets. Significant efforts have been recently devoted to developing low-cost and user-friendly fabrication methods to enable high-density integrations of a large number of droplet generators, some of which are summarized in Table 1. Each method and material has advantages and disadvantages in the preparation of three-dimensional channels for mass production of uniform emulsions. One must consider a variety of factors, such as material compatibility and cost before making a decision on material and process to enable mass production of microfluidic emulsions. The advent of 3D printing and its use in the preparation of three-dimensional channels are extremely exciting developments that warrants continued efforts.

With advances in the design and fabrication of three-dimensional channels, the scale-up of droplet-microfluidics has witnessed significant advances; however, several challenges remain. It is often critical to spatially vary wetting characteristics of channels to enable stable formation of emulsions [73-75]. Thus, it would be imperative to develop methods to spatially pattern wettability in complex channels without complicated procedures. Most scale-up efforts have been focused on the production of simple oil-in-water or

Table 1. Comparison of microfluidic devices manufacturing for high-throughput production of emulsion

Ref.	Material	Microchannel formation	Used equipment	Bonding/ Alignment method	Advantages	Disadvantage
[28,39]	Glass	Dry etching	DRIE (every time)	Thermal fusion bonding/machined support holder	· Good mechanical properties	· Low resolution of droplet generators · Complex and high-cost process
[34]	PMMA	Mechanical cut	CNC milling machine (every time)	Thermal fusion bonding/ Alignment pin	· Three-dimensional stacking · Good mechanical properties	· Low spatial resolution · Complex and high-cost process
[30,31]	PDMS	Photo-/ Soft-lithography	Mask aligner (only once)	Simple O_2 plasma treatment	· Rapid prototyping · Simple bonding and alignment · High resolution channel	· Low mechanical properties · Poor chemical compatibility
		Hybrid Photo-/ Soft-lithography and laser cut	Laser machine (every time)	Stamping and baking of PDMS	· High resolution channel	· Low mechanical properties · Complex process
[72]	Methacrylate photoresist	Digital light processing	3D printer (every time)	-	· Single-step fabrication · Rapid prototyping · Good mechanical properties	· Low spatial resolution

water-in-oil emulsions; however, multiple reports have shown that microfluidics provides unprecedented opportunities in creating complex emulsions such as multiple emulsions [76-78]. There is still a significant room for improvements in the mass production of such complex emulsions. Lastly, as the flow rates that are required to test mass-production devices are expected to increase significantly, fluid delivery systems that can maintain uniform flow rates should be developed. With these advances, droplet-based microfluidics has significant potential in making transformative impact in numerous areas from drug delivery to advanced materials synthesis to high-throughput screening and assay.

ACKNOWLEDGEMENT

We thank SK Innovation Co., LTD. and Berkman Opportunity Fund for support. DI acknowledge support from The University of Pennsylvania and The National Cancer Institute's Innovative Molecular Analysis Technologies program (R21CA182336-01A1).

REFERENCES

1. Y. Kikuchi, K. Sato, H. Ohki and T. Kaneko, *Microvasc. Res.*, **44**, 226 (1992).
2. A. Manz, D. J. Harrison, E. M. J. Verpoorte, J. C. Fettinger, A. Paulus, H. Ludi and H. M. Widmer, *J. Chromatogr.*, **593**, 253 (1992).
3. P. Garstecki, M. J. Fuerstman, H. A. Stone and G. M. Whitesides, *Lab Chip*, **6**, 437 (2006).
4. L. Mazutis and A. D. Griffiths, *Lab Chip*, **12**, 1800 (2012).
5. X. C. I. Solvas and A. deMello, *Chem. Commun.*, **47**, 1936 (2011).
6. S. H. Jin, H. H. Jeong, B. Lee, S. S. Lee and C. S. Lee, *Lab Chip*, **15**, 3677 (2015).
7. Y. Pang, H. Kim, Z. M. Liu and H. A. Stone, *Lab Chip*, **14**, 4029 (2014).
8. S. Sugiura, M. Nakajima, S. Iwamoto and M. Seki, *Langmuir*, **17**, 5562 (2001).
9. A. S. Utada, A. Fernandez-Nieves, H. A. Stone and D. A. Weitz, *Phys. Rev. Lett.*, **99**, 094502 (2007).
10. M. H. Lee, K. C. Hribar, T. Brugarolas, N. P. Kamat, J. A. Burdick and D. Lee, *Adv. Funct. Mater.*, **22**, 131 (2012).
11. H. N. Joensson and H. A. Svahn, *Angew. Chem. Int. Ed.*, **51**, 12176 (2012).
12. H. H. Jeong, S. H. Jin, B. J. Lee, T. Kim and C. S. Lee, *Lab Chip*, **15**, 889 (2015).
13. S. Duraiswamy and S. A. Khan, *Nano Lett.*, **10**, 3757 (2010).
14. J. H. Jung, T. J. Park, S. Y. Lee and T. S. Seo, *Angew. Chem. Int. Ed.*, **51**, 5634 (2012).
15. B. J. Hindson, K. D. Ness, D. A. Masquelier, P. Belgrader, N. J. Heredia, A. J. Makarewicz, I. J. Bright, M. Y. Lucero, A. L. Hiddessen, T. C. Legler, T. K. Kitano, M. R. Hodel, J. F. Petersen, P. W. Wyatt, E. R. Steenblock, P. H. Shah, L. J. Bousse, C. B. Troup, J. C. Mellen, D. K. Wittmann, N. G. Erndt, T. H. Cauley, R. T. Koehler, A. P. So, S. Dube, K. A. Rose, L. Montesclaros, S. L. Wang, D. P. Stumbo, S. P. Hodges, S. Romine, F. P. Milanovich, H. E. White, J. F. Regan, G. A. Karlin-Neumann, C. M. Hindson, S. Saxonov and B. W. Colston, *Anal. Chem.*, **83**, 8604 (2011).
16. S. Juul, Y. P. Ho, J. Koch, F. F. Andersen, M. Stougaard, K. W. Leong and B. R. Knudsen, *ACS Nano*, **5**, 8305 (2011).
17. D. Koziej, C. Floryan, R. A. Sperling, A. J. Ehrlicher, D. Issadore, R. Westervelt and D. A. Weitz, *Nanoscale*, **5**, 5468 (2013).
18. J. J. Agresti, E. Antipov, A. R. Abate, K. Ahn, A. C. Rowat, J. C. Baret,

M. Marquez, A. M. Klibanov, A. D. Griffiths and D. A. Weitz, *Proc. Natl. Acad. Sci. U.S.A.*, **107**, 6550 (2010).
19. E. Brouzes, M. Medkova, N. Savenelli, D. Marran, M. Twardowski, J. B. Hutchison, J. M. Rothberg, D. R. Link, N. Perrimon and M. L. Samuels, *Proc. Natl. Acad. Sci. U.S.A.*, **106**, 14195 (2009).
20. S. L. Sjostrom, Y. P. Bai, M. T. Huang, Z. H. Liu, J. Nielsen, H. N. Joensson and H. A. Svahn, *Lab Chip*, **14**, 806 (2014).
21. M. Muluneh, B. Kim, G. Buchsbaum and D. Issadore, *Lab Chip*, **14**, 4638 (2014).
22. V. Barbier, H. Willaime, P. Tabeling and F. Jousse, *Phys. Rev. E*, **74**, (2006).
23. C. Holtze, *J. Phys. D Appl. Phys.*, **46**, (2013).
24. S. M. Joscelyne and G. Tragardh, *J. Membrane Sci.*, **169**, 107 (2000).
25. G. T. Vladisavljevic, N. Khalid, M. A. Neves, T. Kuroiwa, M. Nakajima, K. Uemura, S. Ichikawa and I. Kobayashi, *Adv. Drug. Deliver. Rev.*, **65**, 1626 (2013).
26. J. Lim, O. Caen, J. Vrignon, M. Konrad, V. Taly and J. C. Baret, *Biomicrofluidics*, **9**, 034101 (2015).
27. S. Sahin and K. Schroen, *Lab Chip*, **15**, 2486 (2015).
28. T. Nisisako, T. Ando and T. Hatsuzawa, *Lab Chip*, **12**, 3426 (2012).
29. M. B. Romanowsky, A. R. Abate, A. Rotem, C. Holtze and D. A. Weitz, *Lab Chip*, **12**, 802 (2012).
30. M. Muluneh and D. Issadore, *Lab Chip*, **13**, 4750 (2013).
31. H. H. Jeong, V. R. Yelleswarapu, S. Yadavali, D. Issadore and D. Lee, *Lab Chip*, **15**, 4387 (2015).
32. D. Bardin, M. R. Kendall, P. A. Dayton and A. P. Lee, *Biomicrofluidics*, **7**, 034112 (2013).
33. W. Li, J. Greener, D. Voicu and E. Kumacheva, *Lab Chip*, **9**, 2715 (2009).
34. D. Conchouso, D. Castro, S. A. Khan and I. G. Foulds, *Lab Chip*, **14**, 3011 (2014).
35. G. Tetradis-Meris, D. Rossetti, C. P. de Torres, R. Cao, G. P. Lian and R. Janes, *Ind. Eng. Chem. Res.*, **48**, 8881 (2009).
36. J. C. McDonald and G. M. Whitesides, *Acc. Chem. Res.*, **35**, 491 (2002).
37. P. N. Nge, C. I. Rogers and A. T. Woolley, *Chem. Rev.*, **113**, 2550 (2013).
38. G. S. Fiorini and D. T. Chiu, *Biotechniques*, **38**, 429 (2005).
39. T. Nisisako and T. Torii, *Lab Chip*, **8**, 287 (2008).
40. Y. Xu, C. X. Wang, L. X. Li, N. Matsumoto, K. Jang, Y. Y. Dong, K. Mawatari, T. Suga and T. Kitamori, *Lab Chip*, **13**, 1048 (2013).
41. J. Kotowski, V. Navratil, Z. Slouka and D. Snita, *Microelectron. Eng.*, **110**, 441 (2013).
42. V. Saarela, M. Haapala, R. Kostiainen, T. Kotiaho and S. Franssila, *Lab Chip*, **7**, 644 (2007).
43. H. Y. Zhai, K. S. Yuan, X. Yu, Z. G. Chen, Z. P. Liu and Z. H. Su, *Electrophoresis*, **36**, 2509 (2015).
44. V. Saarela, M. Haapala, R. Kostiainen, T. Kotiaho and S. Franssila, *J. Micromech. Microeng.*, **19**, 055001 (2009).
45. K. Kolari, V. Saarela and S. Franssila, *J. Micromech. Microeng.*, **18**, (2008).
46. A. Baram and M. Naftali, *J. Micromech. Microeng.*, **16**, 2287 (2006).
47. J. Giboz, T. Copponnex and P. Mele, *J. Micromech. Microeng.*, **17**, R96 (2007).
48. S. Tanzi, M. Matteucci, T. L. Christiansen, S. Friis, M. T. Christensen, J. Garnaes, S. Wilson, J. Kutchinsky and R. Taboryski, *Lab Chip*, **13**, 4784 (2013).
49. P. Abgrall, L. N. Low and N. T. Nguyen, *Lab Chip*, **7**, 520 (2007).
50. D. J. Guckenberger, T. E. de Groot, A. M. D. Wan, D. J. Beebe and E. W. K. Young, *Lab Chip*, **15**, 2364 (2015).
51. M. B. G. Jun, X. Y. Liu, R. E. DeVor and S. G. Kapoor, *J. Manuf. Sci. E-T Asme.*, **128**, 893 (2006).
52. H. Becker and C. Gartner, *Electrophoresis*, **21**, 12 (2000).
53. M. Heckele, A. E. Guber and R. Truckenmuller, *Microsyst. Technol.*, **12**, 1031 (2006).
54. C. W. Tsao and D. L. DeVoe, *Microfluid. Nanofluid.*, **6**, 1 (2009).
55. E. Roy, J. C. Galas and T. Veres, *Lab Chip*, **11**, 3193 (2011).
56. S. C. Yoon, Z. Horita and H. S. Kim, *J. Mater. Process. Tech.*, **201**, 32 (2008).
57. S. C. Yoon, H. G. Jeong, S. Lee and H. S. Kim, *Comp. Mater. Sci.*, **77**, 202 (2013).
58. C. W. Tsao, L. Hromada, J. Liu, P. Kumar and D. L. DeVoe, *Lab Chip*, **7**, 499 (2007).
59. F. Saharil, C. F. Carlborg, T. Haraldsson and W. van der Wijngaart, *Lab Chip*, **12**, 3032 (2012).
60. S. K. Sia and G. M. Whitesides, *Electrophoresis*, **24**, 3563 (2003).
61. W. H. Grover, A. M. Skelley, C. N. Liu, E. T. Lagally and R. A. Mathies, *Sensor. Actuat. B-Chem.*, **89**, 315 (2003).
62. J. W. Zhou, A. V. Ellis and N. H. Voelcker, *Electrophoresis*, **31**, 2 (2010).
63. B. L. Thompson, Y. W. Ouyang, G. R. M. Duarte, E. Carrilho, S. T. Krauss and J. P. Landers, *Nat. Protoc.*, **10**, 875 (2015).
64. F. P. W. Melchels, J. Feijen and D. W. Grijpma, *Biomaterials*, **31**, 6121 (2010).
65. A. Waldbaur, H. Rapp, K. Lange and B. E. Rapp, *Anal. Methods*, **3**, 2681 (2011).
66. A. I. Shallan, P. Smejkal, M. Corban, R. M. Guijt and M. C. Breadmore, *Anal. Chem.*, **86**, 3124 (2014).
67. P. F. O'Neill, A. Ben Azouz, M. Vazquez, J. Liu, S. Marczak, Z. Slouka, H. C. Chang, D. Diamond and D. Brabazon, *Biomicrofluidics*, **8**, 052112 (2014).
68. A. K. Au, W. Lee and A. Folch, *Lab Chip*, **14**, 1294 (2014).
69. G. Comina, A. Suska and D. Filippini, *Lab Chip*, **14**, 424 (2014).
70. C. M. B. Ho, S. H. Ng, K.H. H. Li and Y. J. Yoon, *Lab Chip*, **15**, 3627 (2015).
71. K. C. Bhargava, B. Thompson and N. Malmstadt, *Proc. Natl. Acad. Sci. U. S. A.*, **111**, 15013 (2014).
72. T. Femmer, A. Jans, R. Eswein, N. Anwar, M. Moeller, M. Wessling and A. J. Kuehne, *ACS Appl. Mater. Interfaces*, **7**, 12635 (2015).
73. T. M. Tran, S. Cater and A. R. Abate, *Biomicrofluidics*, **8**, 016502 (2014).
74. L. R. Arriaga, E. Amstad and D. A. Weitz, *Lab Chip*, **15**, 3335 (2015).
75. S. C. Kim, D. J. Sukovich and A. R. Abate, *Lab Chip*, **15**, 3163 (2015).
76. T. Brugarolas, F. Q. Tu and D. Lee, *Soft Matter*, **9**, 9046 (2013).
77. S. S. Datta, A. Abbaspourrad, E. Amstad, J. Fan, S. H. Kim, M. Romanowsky, H. C. Shum, B. J. Sun, A. S. Utada, M. Windbergs, S. B. Zhou and D. A. Weitz, *Adv. Mater.*, **26**, 2205 (2014).
78. C. X. Zhao, *Adv. Drug. Deliver. Rev.*, **65**, 1420 (2013).

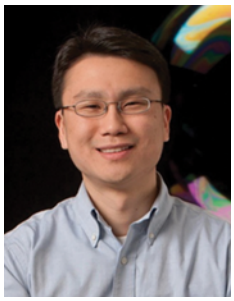

Daeyeon Lee

Daeyeon Lee received his B.S. in Chemical Engineering from Seoul National University in 2001 and received his Ph.D. in Chemical Engineering at MIT in 2007. After his postdoctoral fellowship at Harvard University, Daeyeon joined the University of Pennsylvania in 2009 and is currently Professor of Chemical and Biomolecular Engineering. Daeyeon's research interests include structure-property relationship of nanoparticle assemblies, interfacial behavior of Janus particles, and microfluidic fabrication of functional structures. Daeyeon has won numerous awards including the 2010 Victor K. LaMer Award, NSF CAREER Award, 2012 KIChE President Young Investigator Award, 2013 3M Nontenured Faculty Award, 2013 AIChE NSEF Young Investigator Award and 2014 Unilever Award for Young Investigator in Colloid and Surface Science.